Activation of Methane and Toluene by Rhodium(II) Porphyrin Complexes

Bradford B. Wayland,* Sujuan Ba, and Alan E. Sherry

Department of Chemistry, University of Pennsylvania, Philadelphia, Pennsylvania 19104-6323.
Received October 12, 1990

Abstract: Thermodynamic and kinetic-mechanistic studies are reported for reactions of (tetramesitylporphyrinato)rhodium(II) monomer, (TMP)Rh•, and (tetraxylylporphyrinato)rhodium(II) dimer, $[(TXP)Rh]_2$, with methane that produce hydride and methyl derivatives. A Rh^{II}–Rh^{II} bond energy of ~12 kcal mol^{-1} in $[(TXP)Rh]_2$ was determined by ^1H NMR line broadening and found to dominate differences in the thermodynamic and kinetic parameters for reactions of methane with Rh(II) porphyrins. The sum of the Rh–H and Rh–CH_3 energies is found to be ~117 kcal in both the (TMP)Rh and (TXP)Rh derivatives. Rate laws, activation parameters, and deuterium isotope effects suggest that a four-centered linear transition state (Rh···H_3C···H···Rh) provides a relatively low activation enthalpy route for methane reacting with two metalloradicals. Comparative studies demonstrate that rhodium(II) porphyrins react with toluene exclusively at the benzylic C–H bond, and kinetic studies suggest that this reaction proceeds through a transition state related to that for the methane reactions. Aromatic C–H bond reactions are kinetically excluded for rhodium(II) porphyrins due to steric effects in the transition state.

Introduction

A variety of metal complexes have been observed to react with the C—H unit of methane by oxidative addition to a single metal center,[1-5] σ-bond metathesis of M—X units,[6-8] and addition to M=X groups.[9] We have recently reported a somewhat different type of methane reaction where oxidative addition occurs to two independent metalloradical units.[10] (Tetramesitylporphyrinato)rhodium(II), (TMP)Rh•, reacts selectively with methane in C_6D_6 solvent to form the hydride and methyl derivatives (eq 1).

$$2(TMP)Rh^{\bullet} + CH_4 \underset{k_{-1}}{\overset{k_1}{\rightleftharpoons}} (TMP)Rh\text{–}H + (TMP)Rh\text{–}CH_3 \quad (1)$$

Reaction 1 proceeds by concerted formation of products through a transition state that contains two metalloradicals and methane [(TMP)Rh·CH_4·Rh(TMP)]. This paper presents a more complete description of the kinetic-mechanistic and thermodynamic features of reaction 1, extends the methane reaction studies to (tetraxylylporphyrinato)rhodium(II) dimer, $[(TXP)Rh]_2$, presents comparative studies for alkyl C–H bond reactions of toluene, and explores the origins of the unusual preference of rhodium(II) porphyrins to react with alkane relative to aromatic C–H bonds.

Results

Reactions of Rhodium(II) Porphyrins with Methane in Benzene. (TMP)Rh•. Benzene solutions of (TMP)Rh• react with methane to form equal quantities of (TMP)Rh–CH_3 and (TMP)Rh–H in accord with eq 1. Qualitative evidence for the reversibility of eq 1 is obtained from the observation that benzene solutions containing (TMP)Rh–H and (TMP)Rh–CH_3 at 353 K give reductive elimination to form (TMP)Rh• and CH_4. Reaction 1 proceeds to ^1H NMR observable equilibrium positions at a methane pressure of 1 atm and temperatures of 353, 373, and 393 K. Temperature dependence of the equilibrium constant (K_1) determined by integration of the ^1H NMR spectra (K_1 (353 K) = 7300 ± 700; K_1 (373 K) = 3300 ± 400; K_1 (393 K) = 1100 ± 200) provides thermodynamic values for reaction 1 ($\Delta H_1^0 = -13.0 \pm 1.5$ kcal mol^{-1}; $\Delta S_1^0 = -19 \pm 5$ cal K^{-1} mol^{-1}) (Figure 1). The equilibrium constant at 296 K (P_{CH_4} = 1 atm) was too large to be determined by ^1H NMR. Linearity of kinetic plots of $[(TMP)Rh^{\bullet}]^{-1}$ versus time for more than 3 half-lives at conditions where the methane concentration is held constant and reaction 1 proceeds to virtual completion (T = 296 K; P_{CH_4} = 10 atm; $[CH_4] = 2.35 \times 10^{-1}$ M; $[(TMP)Rh^{\bullet}]_i = 7.0 \times 10^{-4}$ M) indicates that the forward reaction is second order in (TMP)Rh• (Figure 2). Good agreement between the rate constants evaluated on the basis of a third-order process at methane pressures of 1.0 atm (k_1 (296 K) = 0.132 L^2 mol^{-2} s^{-1}) and 10.0 atm (k_1 (296 K) = 0.122 L^2 mol^{-2} s^{-1}) indicates that the reaction is first order in methane (Figures 2 and 3). Plots of $[(TMP)Rh^{\bullet}]^{-1}$ versus time for reaction 1 at 353 and 393 K (P_{CH_4} = 1 atm) are shown in Figure 3. Rate constants at 353 K (k_1 (353 K) = 0.83 L^2 mol^{-2} s^{-1}) and 393 K (k_1 (393 K) = 3.68 L^2 mol^{-2} s^{-1}) were determined from the linear portion of these plots, which occur during the early stages of the reaction. Deviations from linearity become pronounced for the kinetic data at 393 K (Figure 3) as expected for a process approaching equilibrium. Temperature dependence of the forward rate constants (k_1) yields activation parameters for reaction 1 ($\Delta H_1^{\ddagger} = 7.1 \pm 1.0$ kcal mol^{-1}; $\Delta S_1^{\ddagger} = -39 \pm 5$ cal K^{-1} mol^{-1}).

(TMP)Rh• fails to react with neat C_6D_6 or C_6H_6 over a period of months at 353 K. Solutions containing (TMP)Rh–C_6H_5 and (TMP)Rh–H in contact with H_2 (P_{H_2} = 200 Torr) failed to produce any evidence for reductive elimination of benzene over a period of months at 353 K.

$[(TXP)Rh]_2$. Benzene solutions of $[(TXP)Rh]_2$ react reversibly with methane (P_{CH_4} = 1–5 atm) (T = 353–393 K) in accord with eq 2. Proton NMR spectra used in following the progress of reaction 2 are illustrated in Figure 4. Reaction 2 proceeds to an observable equilibrium position (P_{CH_4} = 0.8–1.0 atm; T = 353, 393 K), which permitted evaluation of equilibrium constants by integration of the ^1H NMR spectra (K_2 (353 K) = 0.03 ± 0.01; K_2 (393 K) = 0.04 ± 0.01). The insensitivity of K_2 to temperature

$$[(TXP)Rh]_2 + CH_4 \underset{k_{-2}}{\overset{k_2}{\rightleftharpoons}} (TXP)Rh\text{–}H + (TXP)Rh\text{–}CH_3 \quad (2)$$

changes indicates that ΔH_2^0 is approximately zero ($\Delta H_2^0 \approx 0$ kcal mol^{-1}; $\Delta S_1^0 \approx -7 \pm 3$ cal K^{-1} mol^{-1}). Kinetic data for reaction 2 were obtained by following the loss of $[(TXP)Rh]_2$ at 353 and 393 K (Figure 5). The concentration dependence of the rate can be fitted to a reaction that approaches equilibrium with a rate law in accord with the stoichiometry of reaction 2 ($rate_{f(2)} = k_2[[(TXP)Rh]_2][CH_4]$; $K_2 = k_2/k_{-2}$) (k_2 (353 K) = 0.44 × 101^{-3} L mol^{-1} s^{-1}; K_2 (353 K) = 0.034; k_2 (393 K) = 6.1 × 10^{-3} L mol^{-1}; s^{-1}; K_2 (393 K) = 0.028) (Figure 5). Temperature dependence

(1) (a) Hoyano, J. K.; McMaster, A., Graham, W. A. G. *J. Am. Chem. Soc.* **1983**, *105*, 7190. (b) Rest, A. J.; Whitewell, I.; Graham, W. A. G.; Hoyano, J. K.; McMaster, A. D. *J. Chem. Soc., Chem. Commun.* **1984**, 624. (c) Ghosh, C. K.; Graham, W. A. G. *J. Am. Chem. Soc.* **1983**, *109*, 4726.
(2) Janowicz, A. H.; Bergman, R. G. *J. Am. Chem. Soc.* **1983**, *105*, 3929.
(3) Wenzel, T. T.; Bergman, R. G. *J. Am. Chem. Soc.* **1986**, *108*, 4856.
(4) Hackett, M.; Whitesides, G. M. *J. Am. Chem. Soc.* **1988**, *110*, 1449.
(5) Harper, T. G.; Shinomoto, R. S.; Deming, M. A.; Flood, T. C. *J. Am. Chem. Soc.* **1988**, *110*, 7915.
(6) Watson, P. *J. Am. Chem. Soc.* **1983**, *105*, 6491.
(7) (a) Fendrick, C. M.; Marks, T. J. *J. Am. Chem. Soc.* **1984**, *106*, 2214. (b) Fendrick, C. M.; Marks, T. J. *J. Am. Chem. Soc.* **1986**, *108*, 625.
(8) Thompson, M. E.; Baxter, S. M.; Bulls, A. R.; Burger, B. J.; Nolan, M. C.; Santarsiero, B. D.; Schaefer, W. P.; Bercaw, J. E. *J. Am. Chem. Soc.* **1987**, *109*, 8109.
(9) Cummins, C. C.; Baxter, S. M.; Wolczanski, P. T. *J. Am. Chem. Soc.* **1988**, *110*, 8731.
(10) Sherry, A. E.; Wayland, B. B. *J. Am. Chem. Soc.* **1990**, *112*, 1259.

0002-7863/91/1513-5305$02.50/0

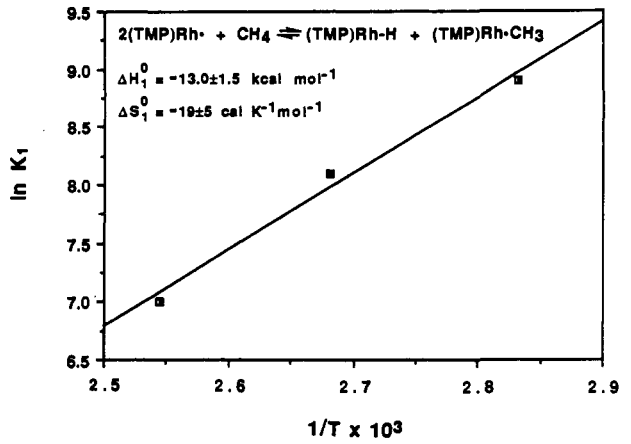

Figure 1. Van't Hoff plot for the reaction of (TMP)Rh• with CH_4 to form (TMP)Rh–H and (TMP)Rh–CH_3 in C_6D_6 solution (K_1 (353 K) = 7300; K_1 (373 K) = 3300; K_1 (393 K) = 1100).

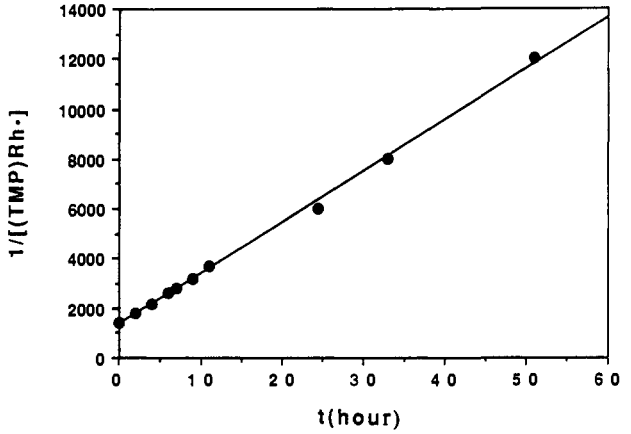

Figure 2. Second-order plot for the reaction of (TMP)Rh• with CH_4 in C_6D_6 at 296 K. ([(TMP)Rh•]$_i$ = 7.02 × 10^{-4} M; 10 atm; P_{CH_4} = 10 atm; [CH_4] = 0.235 M; k_1 = 0.122 L^2 mol^{-2} s^{-1}).

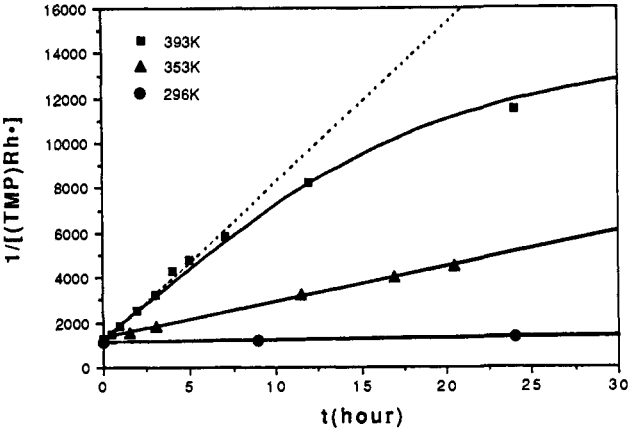

Figure 3. Kinetic studies for reaction 1 in C_6D_6 at a series of temperatures. Points on the graph represent experimental data. Solid lines are calculated for a process that is second order in (TMP)Rh• and first order in CH_4 approaching equilibrium. (■, 393 K, [(TMP)Rh•]$_i$ = 7.90 × 10^{-4} M, [CH_4] = 2.35 × 10^{-2} M, k_1 (393 K) = 3.68 L^2 mol^{-2} s^{-1}, K_1 (393 K) = 1000; ▲, 353 K, [(TMP)Rh•]$_i$ = 7.80 × 10^{-4} M, [CH_4] = 2.45 × 10^{-2} M, k_1 (353 K) = 0.832 L^2 mol^{-2} s^{-1}, K_1 (353 K) = 7300; ●, 296 K, [(TMP)Rh•]$_i$ = 8.85 × 10^{-4} M, [CH_4] = 2.46 × 10^{-2} M, k_1 (296 K) = 0.132 L^2 mol^{-2} s^{-1}).

of the forward rate constants yields values for the activation parameters ($\Delta H_1^{\ddagger}$ = 17 ± 3 kcal mol^{-1}; $\Delta S_1^{\ddagger}$ = −25 ± 7 cal K^{-1} mol^{-1}).

Benzene solutions of (TXP)Rh–H and (TXP)Rh–CH_3 that were prepared by independent routes were observed to reductively eliminate methane with formation of [(TXP)Rh]$_2$ and CH_4 at 353 K. Benzene solutions of [(TXP)Rh]$_2$ are indefinitely stable

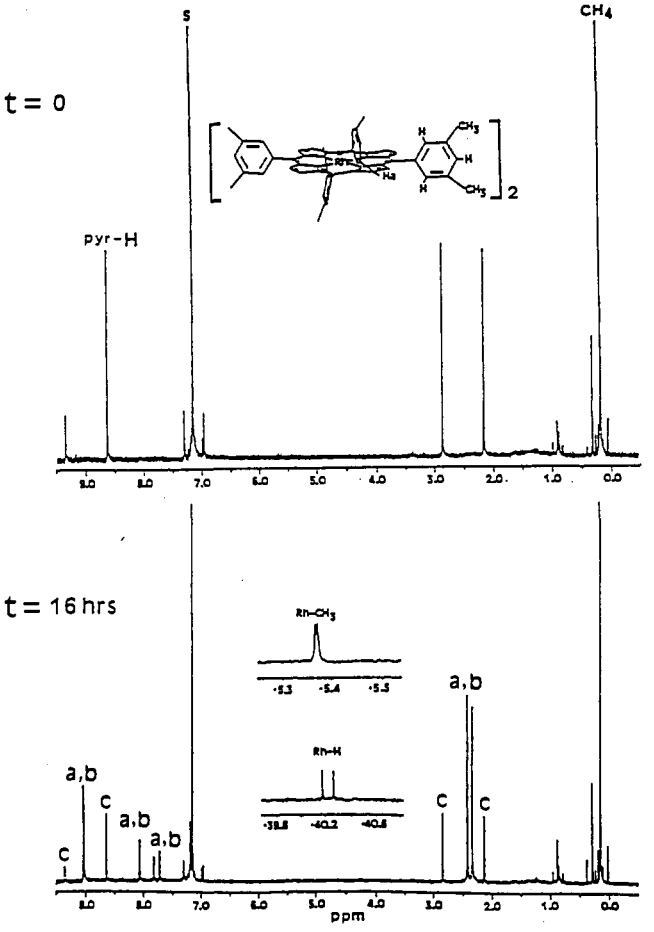

Figure 4. Proton NMR spectra for [(TXP)Rh]$_2$ (4.48 × 10^{-4} M) with CH_4 (P_{CH_4} = 5.18 atm, [CH_4] = 0.1270 M) in C_6D_6: (A) initial spectrum (t = 0), (B) after heating for 16 h at 353 K for (a) (TXP)Rh–H, (b) (TXP)Rh–CH_3, and (c) [(TXP)Rh]$_2$.

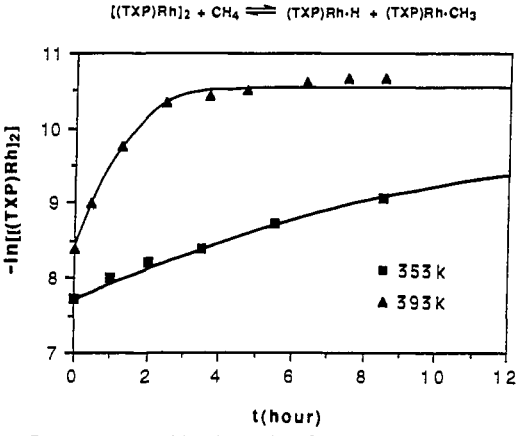

Figure 5. Representative kinetic studies for reaction 2 in C_6D_6 at 353 and 393 K. Points on the graph represent experimental data. Solid lines are calculated for a process that is first order in both [[(TXP)Rh]$_2$ and CH_4 approaching equilibrium. (▲, 393 K, [[(TXP)Rh]$_2$]$_i$ = 2.25 × 10^{-4} M, [CH_4] = 5.36 × 10^{-2} M, k_2 (393 K) = 6.1 × 10^{-3} L mol^{-1} s^{-1}, K_2 (393 K) = 0.028; ■, 353 K, [[(TXP)Rh]$_2$]$_i$ = 4.48 × 10^{-4} M, [CH_4] = 0.1270 M, k_2 (353 K) = 0.44 × 10^{-3} L mol^{-1} s^{-1}, K_2 (353 K) = 0.034).

at 353 K, and solutions containing (TXP)Rh–H and (TXP)Rh–C_6H_5 fail to eliminate benzene over a period of several months at 353 K.

[(OEP)Rh]$_2$. A reexamination of the reaction of [(OEP)Rh]$_2$ with methane in C_6D_6 resulted in observation of the reversible formation of a small quantity of (OEP)Rh–CH_3 and (OEP)Rh–H. The fraction of [(OEP)Rh]$_2$ converted at P_{CH_4} = 8 atm at T = 296 K was insufficient for quantitative kinetic or thermodynamic studies by NMR. Benzene solutions of (OEP)Rh–H and

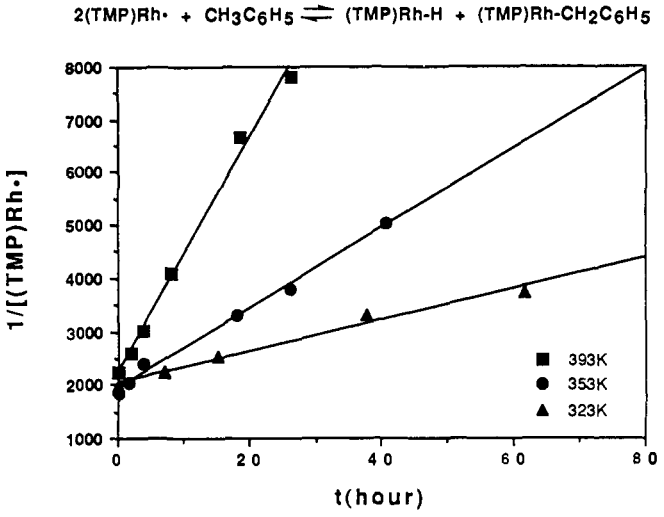

Figure 6. Second-order kinetic plots for reaction 5 in C_6D_6 at a series of temperatures. (■, 393 K, $[CH_3C_6H_5]$ = 0.088 M, $[(TMP)Rh^{\bullet}]_i$ = 4.46 × 10^{-4} M, k_5 (393 K) = 0.35 L^2 mol^{-2} s^{-1}; ●, 353 K, $[CH_3C_6H_5]$ = 0.372 M, $[(TMP)Rh^{\bullet}]_i$ = 5.40 × 10^{-4} M, k_5 (353 K) = 5.50 × 10^{-2} L^2 mol^{-2} s^{-1}; ▲, 323 K, $[CH_3C_6H_5]$ = 0.386 M, $[(TMP)Rh^{\bullet}]_i$ = 5.04 × 10^{-4} M, k_5 (323 K) = 1.04 × 10^{-2} L^2 mol^{-2} s^{-1}).

$(OEP)Rh-CH_3$ readily eliminate methane at 353 K, but $(OEP)Rh-C_6H_5$ failed to react with (OEP)Rh–H with a finite rate at 353 K.

Reactions of Rhodium(II) Porphyrins with Toluene in Benzene. Toluene reacts either as the pure liquid or in benzene solution with each of the Rh(II) porphyrins examined to form equal quantities of the benzyl and hydride complexes (eqs 3–5). There is no evidence for any product of aromatic C–H bond activation. Reaction 3 has been previously reported, and kinetic studies in neat toluene indicated that the reaction is first order in $[(OEP)Rh]_2$.[11]

$$[(OEP)Rh]_2 + CH_3C_6H_5 \rightarrow (OEP)Rh-CH_2C_6H_5 + (OEP)Rh-H \quad (3)$$

$$[(TXP)Rh]_2 + CH_3C_6H_5 \rightarrow (TXP)Rh-CH_2C_6H_5 + (TXP)Rh-H \quad (4)$$

$$2(TMP)Rh^{\bullet} + CH_3C_6H_5 \rightarrow (TMP)Rh-CH_2C_6H_5 + (TMP)Rh-H \quad (5)$$

Kinetics for reaction 5 have been evaluated at a range of conditions ($[CH_3C_6H_5]$ = 0.046–0.372 M; $[(TMP)Rh^{\bullet}]_i$ = (2.10–5.40) × 10^{-4} M; T = 296–393 K). The mole ratio of toluene to (TMP)Rh• was set high enough to ensure that the kinetic behavior is pseudo zero order in toluene. Over the range of conditions studied, reaction 5 proceeds substantially toward completion such that second-order kinetic plots ($[(TMP)Rh^{\bullet}]^{-1}$ vs time) are linear for several half-lives (Figure 6). Satisfactory agreement between rate constants evaluated on the basis of a third-order process at a series of toluene concentrations (0.0465 M toluene (k_5 (353 K) = 6.12 × 10^{-2} L^2 mol^{-2} s^{-1}); 0.0929 M toluene (k_5 (353 K) = 6.47 × 10^{-2} L^2 mol^{-2} s^{-1}); and 0.372 M toluene (k_5 (353 K) = 5.50 × 10^{-2} L^2 mol^{-2} s^{-1})) indicate that reaction 5 is first order in toluene. The rate law for reaction 5 ($rate_{f(5)} = k_5[(TMP)Rh^{\bullet}]^2[CH_3C_6H_5]$) thus has the same form as the reaction of (TMP)Rh• with methane. Temperature dependence of the rate constants provides activation parameters for reaction 5 ($\Delta H_5^{\ddagger}$ = 10.7 ± 1.0 kcal mol^{-1}; $\Delta S_5^{\ddagger}$ = −34 ± 5 cal K^{-1} mol^{-1}) (Figure 7). Kinetic studies with $CD_3C_6D_5$ were used in evaluating the deuterium isotope effect at 353 K ($k_{5(D)}$ (353 K) = 9.3 × 10^{-3} L^2 mol^{-2} s^{-1}) ($k_{5(H)}/k_{5(D)}$ (353 K) = 6.5 ± 0.5).

Estimate of the Rh^{II}–Rh^{II} Bond Energy in $[(TXP)Rh]_2$ from ^1H NMR Line Broadening. Solutions of $[(TXP)Rh]_2$ in benzene have ^1H NMR spectra that broaden dramatically as the temperature is elevated (296–370 K). The line broadening is interpreted as

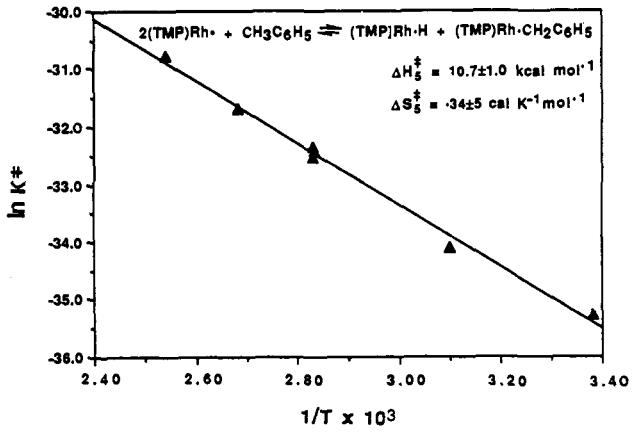

Figure 7. Determination of the activation parameters for reaction 5 in C_6D_6.

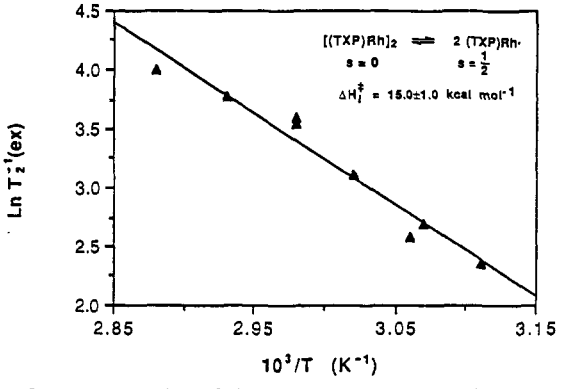

Figure 8. Determination of the activation energy for dissociation of $[(TXP)Rh]_2$ in C_6D_6 by ^1H NMR line broadening.

resulting from exchange of the diamagnetic dimer $[(TXP)Rh]_2$ with the paramagnetic monomer (TXP)Rh• (eq 6). Temperature

$$[(TXP)Rh]_2 \rightleftharpoons 2(TXP)Rh^{\bullet} \quad (6)$$

dependence of the line broadening is analyzed to give the activation enthalpy for dissociation of the dimer by established methodology.[12-14] The contribution of the exchange reaction to the line width at half-height ($\Delta\nu_{1/2}$, $T_2^{-1} = \pi\Delta\nu_{1/2}$) is given by the general expression $T_2^{-1}(ex) = \pi\tau_d^{-1}[(A\tau_p/2)^2][1 + (A\tau_p/2)]^{-1}$ ($T_2^{-1}(ex) = T_2^{-1}(obs) - T_2^{-1}(nat)$) where τ_d and τ_p are the lifetimes for the diamagnetic and paramagnetic species and A is the electron–nuclear coupling constant for the nucleus being observed. The activation enthalpy for the dissociation process ($\Delta H_6^{\ddagger}$) is obtained from the temperature dependence of $T_2^{-1}(ex)$. A plot of ln $T_2^{-1}(ex)$ versus $1/T$ (K) for the pyrrole resonance of $[(TXP)Rh]_2$ is shown in Figure 8 and used in deriving an activation enthalpy of 15.0 ± 1.0 kcal mol^{-1} for reaction 6 ($\Delta H_6^{\ddagger}$ = 15.0 ± 1.0 kcal mol^{-1}). Estimating an activation energy of 3 kcal mol^{-1} for the reverse of reaction 6 yields an estimate of 12 kcal mol^{-1} for the enthalpy of dissociation for $[(TXP)Rh]_2$ ($\Delta H_6^{\circ} \cong$ 12 kcal mol^{-1}). This same method has previously been used in evaluating the activation enthalpy and dissociation energy for homolysis of $[(OEP)Rh]_2$ in benzene ($\Delta H^{\ddagger}$ = 18.5 ± 0.8 kcal mol^{-1}, $\Delta H^{\circ} \approx$ 15.5 ± 0.8 kcal mol^{-1}).[14]

Discussion

Thermodynamic Studies for Methane Activation. Methane reacts with (TMP)Rh• and $[(TXP)Rh]_2$ in benzene to achieve ^1H NMR observable equilibria with the methyl and hydride derivatives (eqs 1 and 2), which can be used in deriving the sum

(11) Del Rossi, K. J.; Wayland, B. B. *J. Am. Chem. Soc.* **1985**, *107*, 7941.

(12) Johnson, C. S., Jr. *Advances in Magnetic Resonance*; Academic Press: New York, 1965; Vol. 1, p 33.

(13) (a) Williams, D. J.; Kreilich, R. W. *J. Am. Chem. Soc.* **1967**, *89*, 3408. (b) Williams, D. J.; Kreilich, R. W. *J. Am. Chem. Soc.* **1968**, *90*, 2775.

(14) Wayland, B. B.; Coffin, V. L.; Farnos, M. D. *Inorg. Chem.* **1988**, *27*, 2745.

of the Rh–H and Rh–CH_3 bond energies. The enthalpy change for the general reaction of a M–M bonded complex with methane (M–M + CH_4 ⇌ M–H + M–CH_3) can be expressed as a set of bond energies (ΔH° = (M–M) + (H_3C–H) – (M–H) – (M–CH_3)). Evaluating this expression by using a H_3C–H bond energy of 105 kcal mol^{-1} [15] and $\Delta H_1^0 = -13$ kcal mol^{-1} provides a value of 118 kcal for the sum of the (TMP)Rh–H and (TMP)Rh–CH_3 bond energies. Using a Rh^{II}–Rh^{II} bond energy of 12 kcal mol^{-1} and $\Delta H_2^0 = 0$ yields 117 kcal for the sum of the (TXP)Rh–H and (TXP)Rh–CH_3 bond energies. These results provide confidence that a self-consistent thermodynamic description of the methane reactions with rhodium porphyrins is emerging. The Rh^{II}–Rh^{II} bond energies in $[(TXP)Rh]_2$ (~12 kcal mol^{-1}) and $[(OEP)Rh]_2$ (~15–16 kcal mol^{-1}) were both estimated from ^1H NMR line broadening studies, and the difference of 3–4 kcal should be highly reliable. $[(OEP)Rh]_2$ reacts with CH_4 in C_6D_6 (353 K) to produce only marginally observable quantities of (OEP)Rh–H and (OEP)Rh–CH_3, which is consistent with the presence of a slightly stronger Rh^{II}–Rh^{II} bond. All of the Rh(II) porphyrins studied have the same type of reaction with methane, and the equilibrium distribution of products varies in a manner consistent with changes in the Rh^{II}–Rh^{II} bond energies.

The sum of the Rh–H and Rh–CH_3 bond energies for the (TMP)Rh and (TXP)Rh derivatives are virtually identical (117–118 kcal mol^{-1}). Reactions of (TMP)Rh$^\bullet$ and $[(TXP)Rh]_2$ with H_2 are too thermodynamically favorable to permit an independent determination of the Rh–H bond energies by NMR methods, and this currently precludes the evaluation of absolute Rh–H and Rh–CH_3 bond energies. IR data suggest that the Rh–H bond energy in (TXP)Rh–H and (TMP)Rh–H may be somewhat smaller than the 62-kcal value observed for (OEP)-Rh–H ($\nu_{(OEP)Rh-H}$ = 2220 cm^{-1}; $\nu_{(TXP)Rh-H} = \nu_{(TMP)Rh-H}$ = 2095 cm^{-1}). Estimating the Rh–H bond energies for (TXP)Rh–H and (TMP)Rh–H at ~60 kcal mol^{-1} places the Rh–CH_3 bond energy at ~57 kcal mol^{-1}.

Kinetic–Mechanistic Studies for Methane Activation. The rate laws for reactions 1 and 2 are compatible with a common transition state that contains two (por)Rh units and methane. Large deuterium isotope effects for reaction 1 ($k_{1(H)}/k_{1(D)}$ (298 K) = 8.6; $k_{1(H)}/k_{1(D)}$ (353 K) = 5.1 ± 0.5) clearly implicate a linear C···H···Rh fragment in the rate-determining step, and the small activation enthalpies ($\Delta H_1^\ddagger$ = 7.1 ± 1.0 kcal mol^{-1}; $\Delta H_2^\ddagger$ = 17 ± 3 kcal mol^{-1}) indicate that the C···H bond breaking in the transition state is accompanied by both Rh···H and Rh···C bond making. These features of the rate-determining process suggest that a linear four-centered transition state as illustrated below guides the subsequent concerted formation of products ((por)-Rh–H, (por)Rh–CH_3).

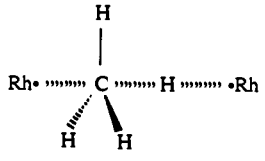

This transition state for oxidative addition of CH_3–H with two separate metalloradicals is complimentary to the three-centered cyclic transition state implicated in oxidative addition to a single metal center.[16,17] Both of these types of transition states synchronize the C–H bond breaking with formation of two bonds, which is necessary when the bond that is being broken (CH_3–H (105 kcal mol^{-1})) is substantially stronger than either of the bonds being formed (Rh–H (~60 kcal mol^{-1}); Rh–CH_3 (~57 kcal mol^{-1})).

Enthalpy profiles constructed from the thermodynamic and activation parameters for reactions of (TMP)Rh$^\bullet$ and $[(TXP)Rh]_2$ with methane appear to differ primarily in that $(TMP)Rh^{II}$ is a monomer and the lowest energy form of $(TXP)Rh^{II}$ is a dimer with a 12 kcal mol^{-1} Rh^{II}–Rh^{II} bond energy. The difference in activation enthalpies ($\Delta H_1^\ddagger$ = 7.1 ± 1.0 kcal mol^{-1}; $\Delta H_2^\ddagger$ = 17 ± 3 kcal mol^{-1}) and activation entropies ($\Delta S_1^\ddagger$ = –39 ± 5 cal K^{-1} mol^{-1}; $\Delta S_2^\ddagger$ = –25 ± 7 cal K^{-1} mol^{-1}) for reactions 1 and 2 are consistent with the dissociation of $[(TXP)Rh]_2$ into monomeric units prior to reaction with the methane substrate.

Formation of a transition state that contains two (por)Rh$^\bullet$ units and CH_4 could occur by a single termolecular step (Scheme I, mechanism A) or a series of bimolecular steps involving an intermediate (mechanism B). Either a metalloradical methane complex [(por)Rh·CH_4] or a metalloradical pair [(por)Rh$^\bullet$ ·Rh(por)] could provide some preorganization for the transition state and function as productive intermediates in pathway B (11a, 11b). The Rh^{II} center in $(por)Rh^{II}$ complexes is not a strong Lewis acid site because the primary acceptor orbital is the half-filled d_{z^2}. Methane is an exceptionally weak donor, and only highly electrophilic metal centers have provided evidence for methane complex formation.[18] Efforts to observe an intermediate methane complex with (TMP)Rh$^\bullet$ have thus far produced only negative results. Binding of methane by a metalloradical like (TMP)Rh$^\bullet$ should be accompanied by changes in the EPR **g** and **A** values as well as contact shifts and shortening of the T_1 and T_2 values for the ^1H and ^{13}C NMR of bulk CH_4 exchanging with coordinated methane.[19] EPR spectra of (TMP)Rh$^\bullet$ in the presence and absence of CH_4 in both toluene and methylcyclohexane glass (90–5 K) are indistinguishable, and both the ^1H NMR shift and relaxation parameters for CH_4 are virtually unaffected by the presence of (TMP)Rh$^\bullet$ in C_6D_6 solvent. While the intermediacy of a methane complex cannot be ruled out, relatively sensitive methods have failed to provide any indication of the perturbation expected for the interaction of a metalloradical with methane. Our continuing effort to obtain evidence for intermediates in reaction 1 is now focused on the observation and potential function of metalloradical dimers.

Scheme I

mechanism A

$$[(por)Rh]_2 \rightleftharpoons 2(por)Rh^\bullet \quad (7)$$

$$2(por)Rh^\bullet + CH_4 \rightleftharpoons [(por)Rh{\cdot}CH_4{\cdot}Rh(por)] \quad (8)$$

$$[(por)Rh{\cdot}CH_4{\cdot}Rh(por)] \rightleftharpoons (por)Rh{-}H + (por)Rh{-}CH_3 \quad (9)$$

mechanism B

$$[(por)Rh]_2 \rightleftharpoons 2(por)Rh^\bullet \quad (10)$$

$$(por)Rh^\bullet + CH_4 \rightleftharpoons [(por)Rh{\cdot}CH_4] \quad (11a)$$

$$[(por)Rh{\cdot}CH_4] + (por)Rh^\bullet \rightleftharpoons [(por)Rh{\cdot}CH_4{\cdot}Rh(por)] \quad (12a)$$

$$2(por)Rh^\bullet \rightleftharpoons [(por)Rh^\bullet\ {}^\bullet Rh(por)] \quad (11b)$$

$$[(por)Rh^\bullet\ {}^\bullet Rh(por)] + CH_4 \rightleftharpoons [(por)Rh{\cdot}CH_4{\cdot}Rh(por)] \quad (12b)$$

$$[(por)Rh{\cdot}CH_4{\cdot}Rh(por)] \rightleftharpoons (por)Rh{-}H + (por)Rh{-}CH_3 \quad (13)$$

Toluene Reactions. Toluene contains both alkyl and aromatic fragments and thus can function as a probe for reaction selectivity between these types of C–H bonds. The methyl group of toluene is observed to react with a series of rhodium(II) porphyrins to produce the hydride and benzyl derivatives (reactions 3–5) without any evidence for aromatic C–H bond activation. The reaction of (TMP)Rh$^\bullet$ with toluene (eq 5) has a rate law ($rate_{f(5)} = k_5[(TMP)Rh^\bullet]^2[CH_3C_6H_5]$) and deuterium isotope effect ($k_{H(5)}/k_{D(5)}$ (353 K) = 6.5 ± 0.5) that are compatible with a transition state analogous to the corresponding methane reaction.

The methyl C–H bonds in toluene are generally considered to be activated relative to those in methane ($PhCH_2$–H = 87 kcal mol^{-1}; CH_3–H = 105 kcal mol^{-1}); however, this is clearly not the

(15) Baghal-Vayjoos, M. H.; Colussi, A. J.; Benson, S. W. *J. Am. Chem. Soc.* **1978**, *100*, 3214.
(16) (a) Janowicz, A. H.; Bergman, R. G. *J. Am. Chem. Soc.* **1982**, *104*, 352. (b) Janowicz, A. H.; Periana, R. A.; Buchanan, J. M.; Kovac, C. A.; Stryker, J. M.; Wax, M. J.; Bergman, R. G. *Pure Appl. Chem.* **1984**, *56*, 13.
(17) Crabtree, R. H. *Chem. Rev.* **1985**, *85*, 245.
(18) Gould, G. L.; Heinekey, D. M. *J. Am. Chem. Soc.* **1989**, *111*, 5502.
(19) Nolan, S. P.; Marks, T. J. *J. Am. Chem. Soc.* **1989**, *111*, 8538.

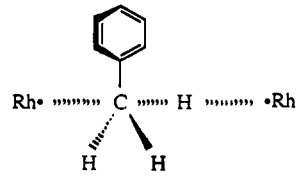

case in the reaction of toluene with (TMP)Rh•, which occurs with a smaller rate (k_1/k_5 (353 K) = 19) and a larger activation enthalpy ($\Delta H_5^{\ddagger}$ = 10.7 kcal mol^{-1}; $\Delta H_1^{\ddagger}$ = 7.1 kcal mol^{-1}). The toluene methyl group is probably deactivated relative to methane in reactions with (TMP)Rh• by increased steric effects in the transition state. We believe that methane reactions with sterically bulky metalloradicals will be kinetically preferred to any larger alkanes. Methane C–H bond reaction may also be thermodynamically favored relative to larger alkanes because of the sensitivity of metal alkyl bond energies to steric effects.

Absence of Aromatic C–H Bond Reactions with Rh(II) Porphyrins. Cationic Rh(III) porphyrins readily react by electrophilic substitution with aromatic molecules to form phenyl derivatives ((por)Rh–C_6H_5).[20] In contrast, rhodium(II) porphyrin complexes are indefinitely stable in benzene, and even heating at 393 K for several weeks fails to produce observable reaction. The ability to examine the reactivity of methane with (TMP)Rh• and $[(TXP)Rh]_2$ in benzene without competitive C–H bond activation with the solvent is currently a unique feature of Rh(II) porphyrin systems but may be generally observed for reactions of sterically bulky metalloradicals.

Oxidative addition of aromatic C–H bonds to single metal centers have invariably been thermodynamically favored over alkane C–H bond reactions because the M–phenyl bond energies have exceeded the M–alkyl bond energies by more than the difference in C–H bond energies.[21-23] Oxidative addition of C–H units to a single metal center usually occurs under thermodynamic rather than kinetic control, which results in a preference for aromatic compared with alkyl C–H bond reactions.[21] In the specific case of rhodium(II) porphyrins, both the oxidative addition of benzene C–H bonds and the reductive elimination of benzene by reaction of (por)Rh–C_6H_5 with (por)Rh–H fail to occur at a finite rate. This is definitive evidence that benzene C–H bond reactions with Rh(II) porphyrins are kinetically inhibited irrespective of the thermodynamics of the reaction. This kinetic effect, which virtually excludes aromatic C–H bond reactions, undoubtedly has its origin in unfavorable interactions between two metalloradicals in the transition state. The structure of benzene precludes attaining a linear Rh•···C···H···•Rh transition state, and the required near tetrahedral angle cannot be accommodated by the sterically bulky metalloradicals.

Cationic Rh(III) porphyrins readily react with benzene and other aromatic C–H groups by electrophilic substitution.[20] The reaction of $(OEP)Rh^+$ with toluene exclusively forms the *p*-tolyl derivative (OEP)Rh–$C_6H_4CH_3$ in preference to alkyl C–H activation. Aromatic substitution is kinetically acceptable because only one rhodium porphyrin occurs in the transition state. Cationic rhodium(III) porphyrin reactions with C–H bonds probably occur with thermodynamic control and have a clear preference for aromatic compared with alkyl C–H bond reactions. Changing from a Rh(II) porphyrin that reacts as a metalloradical to a Rh(III) cationic complex that is a strong electrophile results in changing from kinetic to thermodynamic control of aromatic C–H bond reactions and inversion of the selectivity from alkyl to aromatic C–H bond reactions.

(20) (a) Aoyama, Y.; Tanaka, Y.; Yoshida, T.; Toi, H.; Ogoshi, H. *J. Organomet. Chem.* **1987**, *329*, 251. (b) Aoyama, Y.; Yoshida, T.; Sakurai, K.; Ogoshi, H. *Organometallics* **1986**, *5*, 168.

(21) (a) Jones, W. D.; Feher, F. J. *Acc. Chem. Res.* **1989**, *22*, 91. (b) Jones, W. D.; Feher, F. J. *J. Am. Chem. Soc.* **1984**, *106*, 1650.

(22) (a) Nolan, S. P.; Hoff, C. D.; Stoutland, L. J.; Newman, J. M.; Buchanan, J. M.; Bergman, R. G.; Yang, G. K.; Peters, K. S. *J. Am. Chem. Soc.* **1987**, *109*, 3143. (b) Stoutland, P. D.; Bergman, R. G.; Nolan, S. P.; Hoff, C. D. *Polyhedron* **1988**, *7*, 1429.

(23) (a) Bulls, A. R.; Bercaw, J. E.; Manriquez, J. M.; Thompson, M. E. *Polyhedron* **1988**, *7*, 1409. (b) Dias, A. R.; Simões, J. A. M. *Polyhedron* **1988**, *7*, 1531. (c) Simões, J. A. M.; Beauchamp, J. L. *Chem. Rev.* **1990**, *90*, 629.

Summary and Conclusions

Rhodium(II) porphyrins react with methane in benzene through a probable linear four-centered transition state to form hydride and methyl derivatives. Differences in the thermodynamic and activation parameters for these reactions are dominated by the range of Rh^{II}–Rh^{II} bond energies $[(OEP)Rh]_2$, 15.5 ± 0.8 kcal mol^{-1}; $[(TXP)Rh]_2$, 12.0 ± 0.5 kcal mol^{-1}; (TMP)Rh•, ~0 kcal mol^{-1}). Alkyl C–H bonds in toluene react selectively with Rh(II) porphyrins, and kinetic studies suggest that the toluene and methane alkyl C–H bond reactions proceed by related mechanisms. Aromatic C–H bond reactions are not observed for Rh(II) porphyrins, and this result contrasts with those of cationic Rh(III) porphyrins, which readily react with aromatic C–H bonds by electrophilic substitution. The virtual exclusion of Rh(II) porphyrin activation of aromatic C–H bonds is ascribed to the inability of accommodating two bulky metalloradicals in the near-tetrahedral four-centered transition state required for radical reactions of aromatics. Rhodium(II) porphyrins thus have virtually complete selectivity for alkyl rather than aryl C–H bond reactions, which is in contrast with all other metal complexes that are currently known to activate C–H bonds.

The most important long-range result of this study is recognition that a relatively low activation enthalpy pathway is available for two metalloradicals to react with methane and related saturated hydrocarbons. The trimolecular nature of the transition state associated with these C–H bond reactions is subject to severe steric effects when a nonlinear four-centered array (M···C···H···M) is demanded by the hydrocarbon, and this kinetic effect is manifested in producing virtually total selectivity for alkane versus aromatic C–H bond activation by sterically demanding metalloradicals. This inversion of selectivity from that observed for oxidative addition to single metal centers provides a new dimension for the control of C–H bond reactions.

Experimental Section

General Methods. All manipulations were performed under nitrogen/argon or by vacuum line techniques. NMR data were recorded on either IBM-Bruker WP200SY or Bruker Instruments AF500SY at ambient temperature unless otherwise noted.

Reagents. All reagents were purchased from Aldrich or Strem. $[Rh(CO)_2Cl]_2$ was sublimed prior to use.

Solvents. Deuterated NMR solvents were degassed by freeze–pump–thaw cycles and then refluxed over sodium/benzophenone until the indicator turned purple. Chloroform, methylene chloride, and 1,2-dichloroethane used in synthetic procedures were purified by washing three times with water followed by chromatography on grade 1 alumina for the removal of ethanol and water.

Gases. Research grade methane was purchased from Matheson. CD_4 was purchased from MSD Isotopes and purified by vacuum transferring the contents of the bulb provided by MSD to a new bulb coated with a potassium film. The potassium film was created by gently heating small pieces of potassium metal in the bulb under vacuum.

Preparation of (TMP)Rh Derivatives. (TMP)Rh–I. In a three-neck flask equipped with an addition funnel and a reflux condensor, 250 mg of $Rh_2(CO)_4Cl_2$ dissolved in 40 mL of 1,2-dichloroethane was added dropwise under argon to a suspension containing 375 mg of $(TMP)H_2$ and 300 mg of anhydrous sodium acetate in 200 mL of 1,2-dichloroethane. The resulting solution mixture was then refluxed under argon for 48 h. After cooling to room temperature, I_2 was added in two stages: 100 mg initially and an additional 80 mg after 2 h. The reaction mixture was allowed to stir at room temperature for 3 h following the second addition of I_2. The crude product was concentrated by rotary evaporation after filtration to remove the inorganic salts and chromatographed on grade 3 alumina by using chloroform as the eluent to give the (TMP)-Rh–I in an overall yield of 50–70%. ^{1}H NMR (δ in C_6D_6): 8.83 (pyrrole H, s, 8 H), 2.32 (*o*-CH_3, s, 12 H), 1.75 (*o*′-CH_3, s, 12 H), 7.22 (*m*-H, s, 4 H), 7.05 (*m*′-H, s, 4 H), 2.43 (*p*-CH_3, s, 12 H). FAB MS: m/e = 1010.

(TMP)Rh–CH_3. A 25-mL portion of ethanol and 50 mg of (TMP)-Rh–I were mixed and warmed to 60 °C for 40 min. The resulting solution was then filtered and the filtrate flushed with argon for 30 min. Addition of 7 mg of $NaBH_4$ in 2 mL of aqueous 0.5 M NaOH to the solution under argon caused a color change from red to yellow-brown,

indicating the formation of the (TMP)Rh(I) anion. The resulting solution was then stirred for 30 min. Addition of 0.1 mL of CH_3I resulted in formation of a light orange precipitate, which was collected by filtration. ^1H NMR (δ in C_6D_6): 8.75 (pyrrole H, s, 8 H), 2.26 (*o*-CH_3, s, 12 H), 1.75 (*o'*-CH_3, s, 12 H), 7.20 (*m*-H, s, 4 H), 7.07 (*m'*-H, s, 4 H), 2.43 (*p*-CH_3, s, 12 H), −5.25 (methyl, d, 3 H, $^2J_{^{103}Rh-CH_3}$ = 2.90 Hz). FAB MS: *m/e* = 898.

(TMP)Rh–H. The hydride complex was prepared by using a method similar to that used in the preparation of (TMP)Rh–CH_3 except that acetic acid was added to the (TMP)Rh(I) anion solution instead of CH_3I. ^1H NMR (δ in C_6D_6): 8.77 (pyrrole H, s, 8 H), 2.14 (*o*-CH_3, s, 12 H), 1.79 (*o'*-CH_3, s, 12 H), 7.03 (*m*-H, s, 4 H), 6.95 (*m'*-H, s, 4 H), 2.43 (*p*-CH_3, s, 12 H), −39.99 (hydride, d, 1 H, $^1J_{^{103}Rh-H}$ = 44 Hz). IR (Nujol): ν_{Rh-H} = 2095 cm^{-1}. FAB MS: *m/e* = 884.

(TMP)Rh–C_6H_5. A 10-mL portion of predried benzene was added to a round-bottom flask containing 20 mg of (TMP)Rh–I and 5 mg of $AgSO_3CF_3$, and the contents were stirred under argon at room temperature for 1 h. The product was separated from inorganic salts by filtration and isolated by rotary evaporation of the solvent. ^1H NMR (δ in C_6D_6): 8.76 (pyrrole H, s, 8 H), 2.20 (*o*-CH_3, s, 12 H), 1.70 (*o'*-CH_3, s, 12 H), 2.41 (*p*-CH_3, s, 12 H), 5.34 (*m*-phenyl H, t, 2 H), 4.95 (*p*-phenyl H, t, 1 H), the *m*-H resonance was obscured by the residual solvent peak (7.155), the *o*-phenyl resonance was obscured by other peaks. FAB MS: *m/e* = 960.

(TMP)Rh–$CH_2C_6H_5$. The benzyl complex was prepared by reaction of benzyl bromide with ethanol solutions of (TMP)Rh(I) anion. ^1H NMR (δ in C_6D_6): 8.72 (pyrrole H, s, 8 H), 2.05 (*o*-CH_3, s, 12 H), 1.92 (*o'*-CH_3, s, 12 H), 2.44 (*p*-CH_3, s, 12 H), −3.15 (Rh–$CH_2C_6H_5$, d, 2 H), 3.66 (*o*-H, d, 2 H), 5.78 (*m*-H, dd, 2 H), 6.24 (*p*-H, t, 1 H, $^2J_{^{103}Rh-CH_2Ph}$ = 3.7 Hz).

(TMP)Rh(II). Samples of 0.5–0.8 mg of (TMP)Rh–CH_3 dissolved in 0.5 mL of benzene were irradiated in a Rayonnet photoreactor for 6 h ($\lambda \geq 350$ nm). The products from the reaction were identified as toluene, methane gas, and (TMP)Rh(II). ^1H NMR (δ in C_6D_6 at 296 K): 18.3 (pyrrole H, br s, 8 H), 3.55 (*o*-H, br s, 24 H), 8.87 (*m*-H, br s, 8 H), 3.51 (*p*-H, s, 12 H). EPR (toluene glass at 90 K): $g_\perp$ = 2.65, $g_\parallel$ = 1.915, $A_\perp$ = −197 MHz, $A_\parallel$ = −158 MHz. UV–vis (C_6H_6): λ_{max} = 412, 522 nm. FAB MS: *m/e* = 883.

Preparation of (TXP)Rh Derivatives. 3,5-Dimethylbenzaldehyde. In a two-neck flask containing 5.00 g of mesitylene in 208 mL of a 50% acetic acid solution kept at 80 °C, 91.22 g of $(NH_4)_2Ce(NO_3)_6$ in 416 mL of 50% acetic acid was added dropwise over a period of 1 h.[24] The resulting solution was stirred for 2 h at 80 °C and then cooled to room temperature. The workup of the products was performed by using 250-mL aliquots at a time. Each aliquot was washed four times with a 50:50 ether–pentane mixture. After concentration of the product by rotary evaporation, the solution was neutralized by using sodium carbonate solution and the extraction process outlined above repeated. After rotary evaporation, the residue was washed with cold water, dried over Na_2SO_4, and stored at 5 °C under argon.

After the above procedure was repeated five times, sufficient product was obtained for efficient purification by vacuum fractional distillation. The aldehyde was synthesized in 60% yield. ^1H NMR (δ in $CDCl_3$): 9.92 (aldehyde, s, 1 H), 7.46 (*o*-H, s, 2 H), 7.24 (*p*-H, s, 1 H), 2.37 (*m*-CH_3, s, 6 H).

Tetrakis(3,5-dimethylphenyl)porphyrin. $(TXP)H_2$ was prepared by the condensation of pyrrole with 3,5-dimethylbenzaldehyde in propionic acid according to published procedures.[25] The crude product was then freed of chlorin impurities by established methodology[26] and isolated in ~15% yield. ^1H NMR (δ in C_6D_6): 9.07 (pyrrole H, s, 8 H), 7.85 (*o*-H, s, 8 H), 2.36 (*m*-CH_3, s, 24 H), −2.81 (*n*-H, br s, 2 H), the *p*-H resonance was obscured by the residual solvent peak (7.155). UV–vis (C_6D_6): λ_{max} = 374 nm, 400, 422, 482 (s), 514, 550, 592, 648 nm. FAB MS: *m/e* = 783.

(TXP)Rh–I. In a two-neck flask containing 350 mg of $(TXP)H_2$ and 250 mg of anhydrous sodium acetate suspended in 175 mL of $CHCl_3$, 250 mg of $Rh_2(CO)_4Cl_2$ in 40 mL $CHCl_3$ was added dropwise under argon with use of an addition funnel. The resulting mixture was stirred at room temperature for 5 h, and 100 mg of I_2 was added. After 1 h, another 50 mg of I_2 was added and the mixture allowed to stir for 1 h. The mixture was then filtered for removal of inorganic salts. The filtrate was concentrated and chromatographed on grade 3 alumina by using chloroform as the eluent. ^1H NMR (δ in $CDCl_3$): 8.87 (pyrrole H, s, 8 H), 7.83 (*o*-H, s, 4 H), 7.76 (*o'*-H, s, 4 H), 7.38 (*p*-H, s, 4 H), 2.59 (*m*-CH_3, S, 12 H), 2.53 (*m'*-CH_3, s, 12 H).

(TXP)Rh–CH_3, (TXP)Rh–H, (TXP)Rh–C_6H_5, and (TXP)Rh–$CH_2C_6H_5$. Methyl, hydride, and phenyl derivatives of (TXP)Rh were synthesized following the methodology described for the (TMP)Rh–CH_3, (TMP)Rh–H, and (TMP)Rh–C_6H_5 complexes.

(TXP)Rh–CH_3. ^1H NMR (δ in C_6D_6): 9.02 (pyrrole H, s, 8 H), 8.07 (*o*-H, s, 4 H), 7.82 (*o'*-H, s, 4 H), 2.43 (*m*-CH_3, s, 12 H), 2.34 (*m'*-CH_3, s, 12 H), −5.38 (Rh–CH_3, d, 3 H), the *p*-H resonance was obscured by the residual solvent peak (7.155). FAB MS: *m/e* = 842.

(TXP)Rh–H. ^1H NMR (δ in C_6D_6): 9.03 (pyrrole H, s, 8 H), 8.07 (*o*-H, s, 4 H), 7.72 (*o'*-H, s, 4 H), 2.43 (*m*-CH_3, s, 12 H), 2.34 (*m'*-CH_3, s, 12 H), −40.17 (hydride, d, 1 H, $^1J_{Rh-H}$ = 44 Hz), the *p*-H resonance is obscured by the residual solvent peak (7.155). IR (Nujol): ν_{Rh-H} = 2095 cm^{-1}. FAB MS: *m/e* = 829.

(TXP)Rh–C_6H_5. ^1H NMR (δ in C_6D_6): 9.06 (pyrrole H, s, 8 H), 8.04 (*o*-H, s, 4 H), 7.81 (*o'*-H, s, 4 H), 2.41 (*m*-CH_3, s, 12 H), 2.28 (*m'*-CH_3, s, 12 H), 5.17 (*p*-phenyl H, t, 1 H), 4.92 (*m*-phenyl H, dd, 2 H), the *p*-phenyl H resonance was obscured by the residual solvent peak (7.155), the *o*-phenyl resonance is obscured by other peaks. FAB MS: *m/e* = 904.

[(TXP)Rh]$_2$. Samples of 0.5–0.8 mg of (TXP)Rh–CH_3 dissolved in 0.5 mL of benzene were irradiated in a Rayonnet photoreactor for 6 h ($\lambda \geq 350$ nm). The products from this reaction were identified as toluene, methane gas, and $[(TXP)Rh]_2$. $[(TXP)Rh]_2$ is only sparingly soluble in benzene at room temperature (~1×10^{-4} M), but the solubility increases at elevated temperature (~8×10^{-4} (353 K)). ^1H NMR (δ in C_6D_6): 8.64 (pyrrole H, s, 16 H), 9.35 (*o*-H, s, 8 H), 2.84 (*m*-CH_3, s, 24 H), 2.14 (*m'*-CH_3, s, 24 H), *o'*-H, s, 16 H), 9.35 (*o*-H, s, 8 H), 2.84 (*m*-CH_3, s, 24 H), 2.14 (*m'*-CH_3, s, 24 H), *o'*-H and *p*-H resonances were obscured by the residual solvent peaks. UV–vis: λ_{max} = 408, 522 nm. FAB MS: *m/e* = 828 ((TXP)Rh monomer).

Preparation of (OEP)Rh Derivatives. (OEP)Rh–H, (OEP)Rh–CH_3, $[(OEP)Rh]_2$, and (OEP)Rh–C_6H_5 were prepared by literature methods.[20,27,28]

Kinetic and Thermodynamic Studies. Reactions of hydrocarbons with rhodium(II) porphyrins were carried out in sealed NMR tubes immersed in a constant-temperature bath. Progress of each reaction was evaluated by removing the samples from the bath periodically and recording the ^1H NMR at ambient temperature. Relative concentrations of the rhodium porphyrin species were measured by integration of the ^1H NMR and absolute concentrations measured with respect to a known concentration of methane or toluene as an internal standard. Rate and equilibrium constants measured for independent samples are observed to agree within ~10%, but the absolute error in these parameters could be as large as 30%.

Methane Reactions. All methane reactions were performed in sealed NMR tubes with C_6D_6 solvent. The molar concentration of methane in benzene as a function of temperature and methane pressure is given by the following expression: $[CH_4]_{T,P} = [3.871 \times 10^{-2} \text{ mol } L^{-1} - (5.143 \times 10^{-5})T_2](T_2/T_{1(296)})(P \text{ (1 atm)})$ where P is the CH_4 pressure in atmospheres at temperature T_1 (296 K) and T_2 is the temperature at which the experiment is performed. Solubility data are taken from Evans, F, C.; Battino, R. *J. Chem. Thermodyn.* **1971**, *3*, 753, and the temperature dependence of the density of benzene is from Brunel, R. F.; Van Bibber, K. *Int. Crit. Tables 3*, 27. The solubility of CD_4 in benzene is assumed to be the same as that of CH_4.

(TMP)Rh• with CH_4 and CD_4. Relative concentrations of (TMP)Rh•, (TMP)Rh–H, and (TMP)Rh–CH_3 were determined using ^1H NMR by comparing the integrated intensities of the *p*-CH_3 resonances for the metalloradical with the *o*-CH_3 resonances for the diamagnetic products. Absolute concentrations were obtained by using methane as an internal standard. Accuracy of this method was limited by comparison of broad, overlapping resonances of (TMP)Rh• ($s = {}^1/_2$) with sharp resonances for the diamagnetic complexes (TMP)Rh–H and (TMP)Rh–CH_3.

Equilibrium constants for reaction 1 were determined by proton NMR at 353, 373, and 393 K. The progress of reaction 1 was monitored over a period of at least 7 half-lives and the concentration quotient observed to be constant for a period of at least 2 weeks prior to the final measurements. The solutions investigated had first half-life times between 2 and 10 h, which for a pseudo-second-order process requires reaction times from 15 to 60 days to achieve equilibrium. Repetitive integrations of the ^1H NMR for a single sample at equilibrium give values for the equilibrium constant that vary by less than 10%. Averages of the K values determined by the same procedure for independently prepared samples vary over a range of ~15% (K_1 (353 K) = $(7.3 \pm 0.7) \times 10^3$;

(24) Syper, L. *Tetrahedron Lett.* **1966**, *37*, 4993.
(25) Adler, A. D.; Longo, F. R.; Finarelli, J. D.; Goldmacher, J.; Assour, J.; Korsagoff, L. *J. Org. Chem.* **1967**, *32*, 467.
(26) Groves, J. T.; Nemo, T. E. *J. Am. Chem. Soc.* **1983**, *105*, 6243.
(27) (a) Ogoshi, H.; Setsune, J.; Omura, T.; Yoshida, Z. *J. Am. Chem. Soc.* **1975**, *97*, 6461. (b) Setsune, J.; Yoshida, Z.; Ogoshi, H. *J. Chem. Soc., Perkin Trans. 1* **1982**, 983.
(28) Abeysekera, A. M.; Grigg, R.; Trocka-Grimshaw, J.; Viswanatha, V. *J. Chem. Soc., Perkin Trans. 1* **1977**, 1395.

K_1 (373 K) = (3.3 ± 0.4) × 10^3; K_1 (393 K) = (1.1 ± 0.2) × 10^3).

Kinetic experiments were performed over a range of conditions (P_{CH_4} = 1-10 atm; $[CH_4]$ = (2.4-24) × 10^{-2} M; T = 296-393 K; [(TMP)Rh•] = (6-9) × 10^{-4} M). The methane concentration in solution and the reservoir of methane gas are large compared to the [(TMP)Rh•], which ensures that the observed kinetics for a single sample is pseudo zero order in methane. When the methane concentration is large ($P_{CH_4} \approx 10$ atm) and the temperature relatively low (T = 296 K), reaction 1 proceeds to virtual completion. Plots of $[(TMP)Rh^•]^{-1}$ versus time are linear for more than 3 half-lives, which clearly indicates that reaction 1 is second order in [(TMP)Rh•] ($rate_{f(1)} = -d[(TMP)Rh^•]/2dt = k'[(TMP)Rh^•]^2$). Variation of the methane concentration was used in determining that reaction 1 is first order in methane ($rate_{f(1)} = k[(TMP)Rh^•]^2[CH_4]$). Final analysis of the kinetic data was obtained by simulating the concentration versus time profiles by treating reaction 1 as a third-order process approaching equilibrium and using the experimentally determined equilibrium constants. Simulation of the concentration versus time profiles was obtained by use of the computer program GEAR adapted by T. E. Beukelman and F. G. Weigert from HAVCHM, written by R. N. Stabler and J. Chesick (*Int. J. Chem. Kinet.* **1978**, *10*, 461-469). The PC version (1.1) was converted to Microsoft Fortran (v. 3.31) by R. J. McKinney.

(TMP)Rh• with $CH_3C_6H_5$ and $CD_3C_6D_5$. Stock solutions of $CH_3C_6H_5$ and $CD_3C_6D_5$ (0.100 M) in benzene were prepared in an inert atmosphere box, placed in a vacuum transfer tube, degassed, and stored under argon. Weighed samples of (TMP)Rh-CH_3 were placed into vacuum-adapted NMR tubes, dissolved in benzene, and irradiated in a Rayonnet photoreactor for 6 h ($\lambda \geq 350$ nm) to form (TMP)Rh•. The solvent was then pumped off and 0.5 mL of the toluene stock solution syringed in under argon. The NMR tubes were then attached to a vacuum line and subjected to three freeze-pump-thaw cycles and sealed under vacuum. The samples were subsequently heated in a constant-temperature oil bath, and the concentration of the constituents was periodically monitored by ^{1}H NMR. Linearity of plots for $[(TMP)Rh^•]^{-1}$ versus time and variation of the toluene concentration indicate that the rate law for reaction 5 is second order in [(TMP)Rh•] and first order in toluene ($rate_{f(5)} = k_5[(TMP)Rh^•]^2[CH_3C_6H_5]$).

[(TXP)Rh]$_2$ with CH_4. Relative concentrations of $[(TXP)Rh]_2$, (TXP)Rh-H, and (TXP)Rh-CH_3 were determined by using ^{1}H NMR by comparing the integrated intensities of the pyrrole H resonances of metastable C_6D_6 solutions at 296 K. Three sequential recordings of the spectra demonstrated that the ratio of concentrations remained constant during the time required for data acquisition. Absolute concentrations were obtained by using methane as an internal standard. Kinetic experiments were performed at methane pressures ($P_{CH_4} \approx 1$-6 atm; $[CH_4] \approx (0.24\text{-}1.4) \times 10^{-1}$ M) such that reaction 2 is pseudo zero order in CH_4. Reaction 2 achieves an observable equilibrium position at each of the conditions studied. Equilibrium constants for reaction 2 were evaluated by integration of ^{1}H NMR at equilibrium (K_2 (353 K) = 0.03 ± 0.01; K_2 (393 K) = 0.04 ± 0.01). The combination of experimental error and the complexity associated with a process that achieves observable equilibrium reduces the clarity of defining the rate law. Rate data for reaction 2 are satisfactorily fitted to a process that is first order in both $[(TXP)Rh]_2$ and CH_4 that proceeds to equilibrium, but this description may not be unique. Representative kinetic studies at 1.40 and 5.20 atm of CH_4 illustrate that the rate for reaction 2 can be described as first order in methane at T = 353 K (P_{CH_4} = 1.40 atm, $[CH_4] = 3.55 \times 10^{-2}$ mol L^{-1}, $[(TXP)Rh]_2 = 6.30 \times 10^{-4}$ mol L^{-1}, $k_2' = 1.68 \times 10^{-5}$ s^{-1}, k_2 (353 K) = 4.72 × 10^{-4} mol L^{-1} s^{-1}; P_{CH_4} = 5.18 atm, $[CH_4] = 0.1270$ mol L^{-1}, $[(TXP)Rh]_2 = 4.48 \times 10^{-4}$ mol L^{-1}, $k_2' = 5.64 \times 10^{-5}$ s^{-1}, k_2 (353 K) = 4.44 × 10^{-4} L mol^{-1} s^{-1}). The best fit for the data in Figure 5 for reaction 2 occurring by a process that is first order in both $[(TXP)Rh]_2$ and CH_4 and approaching equilibrium is found for the following rate and equilibrium constants: k_2 (353 K) = 0.44 × 10^{-3} L mol^{-1} s^{-1}, K_2 (353 K) = 0.034; k_2 (393 K) = 6.1 × 10^{-3} L mol^{-1} s^{-1}, K_2 (393 K) = 0.028. The equilibrium constants from analysis of the kinetic data (K_2 (353 K) = 0.034; K_2 (393 K) = 0.028) are in reasonable agreement with the values from integration of ^{1}H NMR at equilibrium (K_2 (353 K) = 0.04 ± 0.01; K_2 (393 K) = 0.03 ± 0.01). The best fit was obtained by using the computer program GIT, written by F. J. Weigert and modified by T. E. Beukelman from HAVCHM (*Int. J. Chem. Kinet.* **1978**, *10*, 461-469).

Acknowledgment. We gratefully acknowledge support of this work by the National Science Foundation through Grant CHE-9014923.

1*H*-Bicyclo[3.1.0]hexa-3,5-dien-2-one. A Strained 1,3-Bridged Cyclopropene

Wolfram Sander,*,† Götz Bucher,† Felix Reichel,‡ and Dieter Cremer*,‡

Contribution from the Institut für Organische Chemie der Technischen Universität, Hagenring 30, D-3300 Braunschweig, FRG, and Department of Theoretical Chemistry, University of Göteborg, Kemigarden 3, S-41296 Göteborg, Sweden. *Received November 27, 1990. Revised Manuscript Received February 19, 1991*

Abstract: Triplet 4-oxocyclohexa-2,5-dienylidene (**5**) gives 1*H*-bicyclo[3.1.0]hexa-3,5-dien-2-one (**4**) on irradiation into its long-wavelength triplet-triplet absorption band (λ = 508-566 nm). Bicyclus **4** was characterized by IR spectroscopy in partially oriented matrices, by deuterium and oxygen-18 isotopic labeling and by comparison of experimental data with ab initio calculations. **4** is highly labile and readily rearranges back to carbene **5** thermally or on visible light (λ = 470 nm) or infrared irradiation. The rates of the thermal **4** → **5** rearrangement have been measured in argon, krypton, xenon, and nitrogen matrices, and deuterium kinetic isotope effects have been determined. The data show that **4** is directly transformed into **5**, with intersystem crossing being rate determining. At low temperatures (<20 K), the rates are independent of temperature, which indicates that the rearrangement occurs via quantum mechanical tunneling. MP2/6-31G(d) calculations show that the cyclopropene ring in **4** is tilted by 129.6° with regard to the cyclopentene ring. The torsional angle between the two carbon 2pπ-orbitals in the cyclopropene ring is 9°, and the pyramidalization angles at C5 are 19.2°. The extra strain energy caused by distortion of the cyclopropene double bond is compensated by the π-stabilization energy of the dienone system. Thus, the total strain energy is only 54 ± 1 kcal/mol—comparable to the strain energy of cyclopropene.

1,3-Bridged cyclopropenes **1** are unstable and highly reactive if the bridge is smaller than n = 6.[1a]

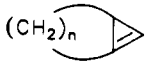

1

While bicyclo[5.1.0]octene (n = 5) slowly dimerizes at room temperature via an ene reaction, bicyclo[4.1.0]heptene (n = 4) is only stable at temperatures below -90 °C. Bicyclo[3.1.0]hexene (n = 3) (**2a**) (Scheme I) has not yet been characterized by spectroscopic methods, but some of its derivatives (**2b-e**) have been trapped in solution.[1]

† Technische Universität Braunschweig.
‡ University of Göteborg.

(1) (a) Billups, W. E.; Haley, M. M.; Lee, G.-A. *Chem. Rev.* **1989**, *89*, 1147. (b) Halton, B.; Bridle, J. H.; Lovett, E. G. *Tetrahedron Lett.* **1990**, *31*, 1313.

0002-7863/91/1513-5311$02.50/0